Key Engineering Materials Vols. 554-557 (2013) pp 99-109
© (2013) Trans Tech Publications, Switzerland
doi:10.4028/www.scientific.net/KEM.554-557.99

Influence of dislocations on the deformability of metallic sheets

Sanda Cleja-Ţigoiu and Raisa Paşcan

University of Bucharest, Romania

e-mail: tigoiu@fmi.unibuc.ro, and tichisanraisa@yahoo.com

Keywords: Finite crystal plasticity. Dislocation density. Hardening variables. Local and non-local evolution equations. Variational problem. Update algorithm. Numerical simulations. Metallic sheets.

Abstract. Within the constitutive framework adopted here, the plastic distortion is described by multislips in the appropriate crystallographic system, the dislocation densities ρ^α and hardening variables ζ^α in the $\alpha-$slip system are the internal variables involved in the model. The rate type boundary value problem at time t leads to an appropriate variational equality to be satisfied by the velocity field when the current state of the body is known. Numerical solutions are analyzed in a tensile problem when only two physical slip systems are activated in the single (fcc) crystal sheet. The slip directions are in the plane of the sheet, while the normals to the slip planes are spatially represented. At the initial moment the distribution of the dislocation density is localized in a central zone of the sheet and in the tensile problem no geometrical imperfection has been introduced. The plane stress state is compatible with the rate type constitutive formulation of the model. The FEM is applied for solving the variational problem in the actual configuration, together with a temporal discretization of the differential system to update the current state in the sheet. The activation condition, which is formulated in terms of Schmid's law, allows us to describe the spread of the plastically deformed zone on the sheet.

Introduction

Defects, such as dislocations, generate plastic permanent deformations and involve changes of the internal structure in crystalline materials, during the deformation process. We adopt the constitutive framework of multiplicative decomposition of the deformation gradient $\mathbf{F}$ into elastic and plastic components, the so-called elastic and plastic distortions,

$$\mathbf{F} = \mathbf{F}^e\mathbf{F}^p \tag{1}$$

within the constitutive framework of finite elasto-plasticity developed in [4]. The material behaves like an orthotropic elastic one with respect to the plastically deformed configurations (the so-called isoclinic configurations). The evolution in time of the plastic distortion is described in the proposed model by multislips in the appropriate crystallographic system, which are also related with the isoclinic configurations. The dislocation densities ρ^α and hardening variables ζ^α in the $\alpha-$slip system are the internal variables involved in the model. The evolution equations for dislocation densities are described either by the local laws like in [8], or by non-local laws, which account for the size effect. For instance, we could consider, the diffusion like evolution equations discussed in [1] and evolution law used in [3], in which the variation in time of the dislocation densities is proportional with the projection of the gradient of the plastic shear rate on the normal and slip directions, respectively. In the numerical example analysed herein, the local evolution equations for the dislocation densities have been considered only. The rate type boundary value problem at time t leads to an appropriate variational equality to be satisfied by the velocity field when the current state of the body, namely the Cauchy stress, position of the slip systems, dislocation densities and hardening variables are known. We invoke the compatibility of the in-plane stress state with the constitutive model when only two slip systems could be activated. The FEM is applied for solving the variational problem to define the velocity field in the actual configuration, together with a temporal discretization of the differential

All rights reserved. No part of contents of this paper may be reproduced or transmitted in any form or by any means without the written permission of TTP, www.ttp.net. (ID: 193.136.169.123, Technical University of Cluj Napoca, Cluj Napoca, Romania-23/04/13,15:11:12)

system (which defines the rate type of the constitutive equations) to update the current state in the sheet. By using the Matlab program, we solve numerically the problem concerning the deformation of the sheet made up from a single (fcc) crystal when only two physical slip systems could be activated. For the FEM procedure we make reference to [13, 14]. At the initial moment, a non-homogeneous distribution of the scalar dislocation density is assumed in the sheet. The spread on the sheet of the plastically deformed zone in time is numerically emphasized, starting from the reference configuration. The activation condition of the slip systems is the key point in describing the variation in time of the plastically deformed zone, plastic shears and dislocation density. No geometrical imperfections have been considered and the slip systems are physically accepted for a (fcc) single crystal.

Constitutive model with dislocation

The material behaves like an elastic one with respect to the plastically deformed configurations (the so-called isoclinic configurations), with the Cauchy stress, $\mathbf{T}$, expressed in terms of the elastic strain, $\mathbf{E}^e$, by

$$\frac{\mathbf{T}}{\hat{\rho}} = \mathcal{E}\mathbf{E}^e \quad \text{with} \quad \mathbf{E}^e = \frac{1}{2}\left((\mathbf{F}^e)^T\mathbf{F}^e - \mathbf{I}\right). \tag{2}$$

In our consideration, $\mathcal{E}$ characterizes the elastic compliance matrix in the actual configuration which is derived from the matrix of cubic (orthotropic) elastic material, $\mathcal{C}$, with the coefficients given with respect to the isoclinic configuration by the pushing away procedure, namely

$$\begin{aligned} &\mathcal{E}[\mathbf{X}] = \mathbf{F}^e(\mathcal{C}\left[(\mathbf{F}^e)^T\mathbf{X}\mathbf{F}^e\right])(\mathbf{F}^e)^T, \quad \forall\mathbf{X} \text{ symmetric tensor} \\ &\mathcal{E}_{ijkl} = F^e_{im}F^e_{jn}F^e_{ks}F^e_{lr}\mathcal{C}_{mnsr}, \quad \text{(Euler notation)} \end{aligned} \tag{3}$$

The matrix $\mathcal{C}$ is characterized by only three elastic material constants as can be seen in Ting [10], $\mathcal{C}_{11} = \mathcal{C}_{22} = \mathcal{C}_{33}, \mathcal{C}_{12} = \mathcal{C}_{13} = \mathcal{C}_{23}, \mathcal{C}_{44} = \mathcal{C}_{55} = \mathcal{C}_{66}$, using the standard notation with two indices.

In the proposed model, the evolution in time of the plastic distortion is described by multislips in the appropriate crystallographic system

$$\dot{\mathbf{F}}^p\,(\mathbf{F}^p)^{-1} = \sum_{\alpha=1}^{N}\nu^\alpha(\bar{\mathbf{s}}^\alpha \otimes \bar{\mathbf{m}}^\alpha), \tag{4}$$

where ν^α are the plastic shear rates in the slip system α. The slip system, initially given in the isoclinic configuration, where $\bar{\mathbf{m}}^\alpha$ is the normal to the slip plane and $\bar{\mathbf{s}}^\alpha$ is the slip direction, is further deformed due to the presence of the elastic distortion $\mathbf{F}^e$. In the actual configuration, the slip system is defined through the formulae

$$\mathbf{F}^e\bar{\mathbf{s}}^\alpha = \mathbf{s}^\alpha, \quad (\mathbf{F}^e)^{-T}\,\bar{\mathbf{m}}^\alpha = \mathbf{m}^\alpha. \tag{5}$$

The orthogonality condition $\mathbf{s}^\alpha \cdot \mathbf{m}^\alpha = 0$ obviously holds.

By taking the time derivative of the multiplicative relation (1), the rate of elastic distortion can be expressed in the actual configuration, in terms of the velocity gradient $\mathbf{L} = \nabla\mathbf{v}$, as

$$\dot{\mathbf{F}}^e\,(\mathbf{F}^e)^{-1} = \mathbf{L} - \sum_{\alpha=1}^{N}\nu^\alpha\,(\mathbf{s}^\alpha \otimes \mathbf{m}^\alpha), \quad \mathbf{L} = \dot{\mathbf{F}}\,(\mathbf{F})^{-1}, \tag{6}$$

where **v** denotes the the spatial velocity.

The model will be strongly related to the presence of dislocations inside the body and the production, annihilation and motion of the dislocations. The following internal variables are used herein: the dislocation densities ρ^α and hardening variables ζ^α in the $\alpha-$slip system.

The activation condition is formulated in terms of the Schmid's law, i.e.

$$|\tau^\alpha| \geq \zeta^\alpha \quad \Longleftrightarrow \quad \mathcal{F}^\alpha \geq 0 \quad \text{where} \quad \mathcal{F}^\alpha := |\tau^\alpha| - \zeta^\alpha, \tag{7}$$

with

$$\tau^\alpha = \boldsymbol{\tau}\mathbf{m}^\alpha \cdot \mathbf{s}^\alpha. \tag{8}$$

and

$$\boldsymbol{\tau} = J\mathbf{T}, \qquad J = \det\mathbf{F} \quad \text{şi} \quad J\hat{\rho} = \hat{\rho}_0. \tag{9}$$

Here, $\hat{\rho}$ and $\hat{\rho}_0$ denote the mass densities in the actual and reference configurations, respectively.

A viscoplastic flow rule associated with the deformation process is given under the following form in [9]

$$\nu^\alpha = \dot{\gamma}^\alpha = \dot{\gamma}_0^\alpha \left|\frac{\tau^\alpha}{\zeta^\alpha}\right|^n \text{sign}(\tau^\alpha)\mathcal{H}(\mathcal{F}^\alpha), \quad \forall\alpha = 1, ..., N. \tag{10}$$

The hardening law is described either as a given function dependent on the dislocation densities, e.g. $\zeta^\alpha = \mu b \left(\sum_\beta a^{\alpha\beta}\rho^\beta\right)^{1/2}$ [9], where μ is the elastic shear modulus, b is the magnitude of the Burgers vector, $a^{\alpha\beta}$ is the matrix taking into account various types of dislocation interactions, or by an evolution law proposed like in crystal plasticity in terms of plastic shear rates [8]

$$\dot{\zeta}^\alpha = \sum_{\beta=1}^{N} h^{\alpha\beta}\left|\dot{\gamma}^\beta\right|. \tag{11}$$

Here $h^{\alpha\beta} = h^{\alpha\beta}(\rho^q)$ are the components of the hardening matrix and they depend on the dislocation density. Moreover this matrix has been represented by Teodosiu [8] as

$$h^{\alpha\beta} = \frac{\mu}{2}a^{\alpha\beta}\left(\sum_q a^{\alpha q}\rho^q\right)^{-1/2}\left\{\frac{1}{K}\left(\sum_{q\neq\alpha}\rho^q\right)^{1/2} - 2y_c\rho^\alpha\right\}, \tag{12}$$

where K is a material parameter and y_c denotes a characteristic length associated with the annihilation process of dislocation dipolles.

The evolution in time of the dislocation densities are described either by a local evolution equation, or by non-local laws, which account for the size effect.

I. We consider the local evolution equation, say of the type given in [8]

$$\dot{\rho}^\alpha = \frac{1}{b}\left(\frac{1}{L^\alpha} - 2y_c\rho^\alpha\right)|\nu^\alpha| \quad \text{cu} \quad L^\alpha = K\left(\sum_{q\neq\alpha}\rho^q\right)^{-1/2}. \tag{13}$$

II. A non local evolution equation, namely a diffusive evolution equation, [1], which is non-linear of the parabolic type

$$\dot{\rho}^{\alpha} = D\left(k\Delta\rho^{\alpha} - \frac{\partial\psi_T}{\partial\rho^{\alpha}}\right)|\nu^{\alpha}|, \quad \alpha = 1,\ldots,N, \tag{14}$$

where D and k are material constants. Here, Ψ_T represents the defect energy.
Remark. We could identify the appropriate expression for the potential ψ_T by considering the equality between the functions occurring in the right hand side of equations (13) and (14) in which we take $k = 0$.

III. The evolution law used in [2] asserts the variation in time of the dislocation densities is proportional with the projection of the gradient of the plastic shear rate on the normal and slip direction, respectively. A non-local evolution equation for the dislocation density dependent on its gradient has been derived in [7].

The initial conditions have to be attached to the differential system, while a boundary condition has to be defined in connection with the partial differential equation (14). For instance, one can consider the following boundary condition

$$k\frac{\partial\rho^{\alpha}}{\partial\mathbf{n}} = i^{\alpha}\left(\rho^{q}\right) \tag{15}$$

with $i^{\alpha}\left(\rho^{q}\right)$ given functions that could depend on the scalar dislocation density, and could be influenced by the shape of the boundary domain. Such type of boundary condition has been introduced in [1, 7].

Variational problem

The weak formulation associated with the balance equation at time t can be emphasized using an update Lagrangian formalism (see [6, 12]), or a principle of the virtual power (see [8, 3])

If the activation condition is formulated in terms of Schmid's law, the rate type boundary value problem at time t leads to an appropriate variational equality to be satisfied by the velocity field, $\mathbf{v}$, when the current state of the body, namely the Cauchy stress, $\mathbf{T}$, position of the slip systems, $(\mathbf{m}^{\alpha}, \mathbf{s}^{\alpha})$, dislocation densities , ρ^{α}, and hardening variables, ζ^{α}, are known. We obtain

$$\begin{aligned}
&\int_{\Omega_t}(\nabla\mathbf{v})\mathbf{T}\cdot\nabla\mathbf{w}d\mathbf{x} + \int_{\Omega_t}\hat{\rho}\mathcal{E}[\mathbf{D}]\cdot\nabla\mathbf{w}d\mathbf{x} - \\
&-\sum_{\alpha=1}^{N}\int_{\Omega_t}\nu^{\alpha}\{\hat{\rho}\mathcal{E}\left[\left\{\mathbf{s}^{\alpha}\otimes\mathbf{m}^{\alpha}\right\}^{\mathsf{S}}\right] + \left(\mathbf{s}^{\alpha}\otimes\mathbf{m}^{\alpha}\right)\mathbf{T} + \mathbf{T}\left(\mathbf{s}^{\alpha}\otimes\mathbf{m}^{\alpha}\right)^{T}\cdot\nabla\mathbf{w}d\mathbf{x} = \\
&= \int_{\Gamma_{1t}}\dot{\mathbf{s}}_t\cdot\mathbf{w}da + \int_{\Omega_t}\rho\dot{\mathbf{b}}_t\cdot\mathbf{w}d\mathbf{x}, \quad \forall\mathbf{w}\in\mathcal{V}_{ad}
\end{aligned} \tag{16}$$

with

$$\nu^{\alpha} = J\,\nu_0^{\alpha}\left|\frac{\mathbf{T}\,\mathbf{m}^{\alpha}\cdot\mathbf{s}^{\alpha}}{\zeta^{\alpha}}\right|^{n} sign\left(\mathbf{T}\mathbf{m}^{\alpha}\cdot\mathbf{s}^{\alpha}\right)\mathcal{H}\left(\mathcal{F}^{\alpha}\right), \quad \alpha = 1,\ldots,N. \tag{17}$$

The finite element method (FEM) is applied for solving the variational problem to define the velocity field in the actual configuration, $\mathbf{v}$, together with a temporal discretization of the differential system (which defines the rate type of the constitutive equations) to update the current state in the sheet.

In-plane stress state with two slip systems only

Under the hypothesis that the stress state is developed during the deformation process, either the components $T_{3j}, j = 1, 2, 3$ vanish, or $\dfrac{d}{dt}\left(\dfrac{T_{3j}}{\hat{\rho}}\right) = 0, j = 1, 2, 3.$

Moreover the velocity field could be represented by $v_1 = v_1(x_1, x_2), v_2 = v_2(x_1, x_2)$, and v_3 chosen to be compatible with the stress state.

The following consequences obtained within the framework formulated in the section 2.

Proposition 1. 1. The elastic type constitutive equation associated with the orthotropic cubic material is compatible with the in-plane stress state if and only if the elastic distortion is given by

$$\mathbf{F}^e = \begin{pmatrix} F^e_{11} & F^e_{12} & 0 \\ F^e_{21} & F^e_{22} & 0 \\ 0 & 0 & F^e_{33} \end{pmatrix}. \tag{18}$$

2. The plastic distortion allows a similar peculiar form , namely

$$\mathbf{F}^p = \begin{pmatrix} F^p_{11} & F^p_{12} & 0 \\ F^p_{21} & F^p_{22} & 0 \\ 0 & 0 & F^p_{33} \end{pmatrix}. \tag{19}$$

For the sake of simplicity, we assume that only two slip systems can become active. For a face cubic centered slip system, we are restricted to the following slip systems

$$\begin{aligned} \mathbf{s}^1 &= \frac{1}{\sqrt{2}}\left[1, \bar{1}, 0\right], \quad \mathbf{m}^1 = \frac{1}{\sqrt{3}}\left(1, 1, 1\right) \\ \mathbf{s}^7 &= \frac{1}{\sqrt{2}}\left[1, \bar{1}, 0\right], \quad \mathbf{m}^7 = \frac{1}{\sqrt{3}}\left(\bar{1}, \bar{1}, 1\right) \end{aligned} \tag{20}$$

which have been labeled following the list of slip systems to be found in Bortoloni and Cermelli [1], see also [5].

Thus it can be proven that $\dfrac{d}{dt}\left(\dfrac{T_{3j}}{\hat{\rho}}\right)$ vanish for $j = 1, 2$ within the adopted constitutive framework. Moreover, the rate of plastic distortion is characterized by

$$\dot{\mathbf{F}}^p \left(\mathbf{F}^p\right)^{-1} = \nu^1(\bar{\mathbf{s}}^1 \otimes \bar{\mathbf{m}}^1 - \bar{\mathbf{s}}^7 \otimes \bar{\mathbf{m}}^7) \tag{21}$$

since $\nu^1 = -\nu^7$ and $|\tau^1| = |\tau^7|$.

Proposition 2. The restriction $\dfrac{d}{dt}\left(\dfrac{T_{33}}{\hat{\rho}}\right) = 0$ imposed on the stress state could be accomplished if and only if D_{33} is given by

$$\begin{aligned} D_{33} \;&= \frac{1}{\mathcal{E}_{33}}(-\mathcal{E}_{31}D_{11} - \mathcal{E}_{32}D_{22} - 2\mathcal{E}_{34}D_{12} + \\ &+\mathcal{E}_{31}G^S_{11} + \mathcal{E}_{32}G^S_{22} + \mathcal{E}_{33}G^S_{33} + 2\mathcal{E}_{34}G^S_{12}) \\ &\text{where} \quad G_{kl} = \sum_{\alpha=1,7} \nu^\alpha s^\alpha_k m^\alpha_l, \quad \mathbf{G}^S = \frac{1}{2}(\mathbf{G} + \mathbf{G}^T). \end{aligned} \tag{22}$$

In the case considered herein, $G_{13} = G_{23} = G_{31} = G_{32} = 0$.

Finite element discretization

The solution of the variational problem (16), which has been formulated at the time moment t, is obtained by the FEM. Let us consider $(t_n)_{n=1,N}$ be a partition of the time interval $[0,T]$ with $t_{n+1} = dt + t_n$. We assume that the current values of the fields are known at moment t_n, i.e.

$$\mathbf{T}_n/\hat{\rho}_n, \mathbf{F}_n^e, \mathbf{s}_n^\alpha, \mathbf{m}_n^\alpha, \gamma_n^\alpha, \rho_n^\alpha, \zeta_n^\alpha. \tag{23}$$

Let Ω_{t_n} be the domain occupied by the body at time t_n. We rewrite the variational problem at time t_n to be satisfied by the velocity field $\mathbf{v}$:

$$\begin{aligned} &\textstyle\int_{\Omega_{t_n}} (\nabla \mathbf{v})\mathbf{T} \cdot \nabla \mathbf{w} d\mathbf{x} + \int\limits_{\Omega_{t_n}} \hat{\rho}\mathcal{E}\left[\mathbf{D}\right] \cdot \nabla \mathbf{w} d\mathbf{x} - \int\limits_{\Omega_{t_n}} \left\{\hat{\rho}\mathcal{E}\left[\mathbf{G}^S\right] + \mathbf{GT} + \mathbf{TG}^{\mathsf{T}}\right\} \cdot \nabla \mathbf{w} d\mathbf{x} = \\ &= \int\limits_{\Gamma_{1t_n}} \dot{\mathbf{s}}_t \cdot \mathbf{w} da + \int\limits_{\Omega_{t_n}} \rho \dot{\mathbf{b}}_t \cdot \mathbf{w} d\mathbf{x}, \quad \forall \mathbf{w} \in \mathcal{V}_{ad}. \end{aligned} \tag{24}$$

The finite elements are chosen to be triangles and the shape functions are considered to be linear over each element. By applying the classical FEM the discretized variational equality can be written in the following matrix representation

$$\begin{aligned} &\tilde{\mathbf{K}}\tilde{\mathbf{v}} = -\bar{\mathbf{K}}\bar{\mathbf{v}} + \mathbf{f}, \\ &\text{where} \\ &\tilde{\mathbf{K}} = \sum_e (\tilde{\mathbf{A}}^e)^T \mathbf{K}^e \tilde{\mathbf{A}}^e, \quad \bar{\mathbf{K}} = \sum_e (\tilde{\mathbf{A}}^e)^T \mathbf{K}^e \bar{\mathbf{A}}^e, \quad \mathbf{f} = \sum_e (\tilde{\mathbf{A}}^e)^T \mathbf{f}^e. \end{aligned} \tag{25}$$

Here $\tilde{\mathbf{v}}$ is the vector built using the components of the velocitiy in all network points at the nodes except those which lying on the part of the boundary where velocities are imposed. On the contrary, the vector $\bar{\mathbf{v}}$ contains the components of the velocities at the FEM global nodes where velocity is prescribed. We write the expressions for the elements from formulae (25):

$$\mathbf{K}^e = \left(\mathbf{B}_2^{eT}\mathbf{B}_1^e + \hat{\rho}\mathbf{B}_4{}^{eT}\mathcal{E}\mathbf{B}_3^e\right)\mathcal{A}^e \tag{26}$$

$$\mathbf{f}^e = \left(\hat{\rho}\mathbf{B}_4^{eT}\mathcal{E}\mathbf{G}^S - \mathbf{B}_4^{eT}\mathcal{E}\mathbf{q} + \mathbf{B}_4^{eT}\mathbf{Q}\right)\mathcal{A}^e + \int\limits_{\partial\Omega_{t_n}^e \cap \partial\Omega_{t_n}} \mathbf{N}^e \dot{\mathbf{s}}_t da, \tag{27}$$

$$\mathbf{B}_1^e = \Delta_1 \mathbf{N}^{eT}, \mathbf{B}_2^e = \Delta_2 \mathbf{N}^{eT}, \mathbf{B}_3^e = \Delta_3 \mathbf{N}^{eT}, \mathbf{B}_4^e = \Delta_4 \mathbf{N}^{eT}. \tag{28}$$

$$\mathbf{N}^{eT} = \begin{bmatrix} N_1^e & 0 & N_2^e & 0 & N_3^e & 0 \\ 0 & N_1^e & 0 & N_2^e & 0 & N_3^e \end{bmatrix} \tag{29}$$

$$\mathcal{E} = \begin{pmatrix} \mathcal{E}_{11} & \mathcal{E}_{12} & \mathcal{E}_{13} & \mathcal{E}_{14} \\ \mathcal{E}_{21} & \mathcal{E}_{22} & \mathcal{E}_{23} & \mathcal{E}_{24} \\ \mathcal{E}_{41} & \mathcal{E}_{42} & \mathcal{E}_{43} & \mathcal{E}_{44} \end{pmatrix}, \quad \mathbf{G}^S = \begin{Bmatrix} G_{11}^S \\ G_{22}^S \\ G_{33}^S \\ G_{12}^S \end{Bmatrix}, \tag{30}$$

$$\mathbf{q} = \left\{ \begin{array}{c} 0 \\ 0 \\ \dfrac{1}{\mathcal{E}_{33}} \left\{ \mathcal{E}_{31} G^S_{11} + \mathcal{E}_{32} G^S_{22} + \mathcal{E}_{33} G^S_{33} + 2\mathcal{E}_{34} G^S_{12} \right\} \\ 0 \end{array} \right\}, \tag{31}$$

$$\mathbf{Q} = \left\{ \begin{array}{c} 2(G_{11}T_{11} + G_{12}T_{21}) \\ 2(G_{21}T_{12} + G_{22}T_{22}) \\ G_{11}T_{12} + G_{12}T_{22} + G_{21}T_{11} + G_{22}T_{21} \end{array} \right\}. \tag{32}$$

Here $\mathcal{A}^e$ denotes the measure of the surface associate with the finite element e in the deformed configuration at moment t_n, while $\Delta_1, \Delta_2, \Delta_3$ and Δ_4 are appropriate differential operators.

When the velocity field **v** has been numerically found at time t_n the velocity gradient, **L**, and rate of strain, **D**, follow at once, and further by applying an update procedure to the appropriate differential-like relationships associated with the constitutive equations describing the model, namely an explicit Euler algorithm, we provide the values at time t_{n+1} for the fields listed in (23).

Note that at this level of computation only the *local type* of the evolution equations, say (13), have been considered. When the non-local evolution equations for the dislocation densities have to be taken into account, then a weak form of these equations ought to be introduced, see e.g. Kuroda [3] or in [7], and then numerically solved.

Numerical solutions

We solve numerically the problem consisting of the deformation of a strip of length L_0 in the direction of the axis X_1 and length l_0 in the direction X_2, respectively, when velocity is imposed at the ends of this strip

$$\left\{ \begin{array}{lll} v_1 = 0,\ (\dot{s}_t)_2 = 0 & \text{along} & X_1 = 0, \forall X_2 \in [0, L_0] \\ v_1 = v_1^*,\ (\dot{s}_t)_2 = 0 & \text{along} & X_1 = L_0, \forall X_2 \in [0, L_0] \\ v_2 = 0 & \text{in} & X_1 = X_2 = 0 \quad \text{and} \quad X_1 = L_0,\ X_2 = 0. \end{array} \right. \tag{33}$$

As can be seen from Fig. 1, $X_2 = 0$ and $X_2 = l_0$ are stress free boundaries, namely $(\dot{s}_t)_1 = 0, (\dot{s}_t)_2 = 0$, for all $X_1 \in (0, L_0)$.

The prescribed displacement rate is given by $v_1^* = 5 \cdot 10^{-3}$mm/s.

Note that the physical slip systems considered have the slip directions in the plane of the sheet, but the corresponding normal has a spatial representation.

The initial densities of dislocation are given by the function

$$\rho_0^\alpha(X_1, X_2) = \left\{ \begin{array}{ll} \rho_{max} & \exp\big(-\dfrac{1}{R^2} ln(\rho_{min}/\rho_{max}) \big((X_1 - X_1^0)^2 + (X_2 - X_2^0)^2 - R^2 \big) \big), \\ & \text{for} \quad (X_1 - X_1^0)^2 + (X_2 - X_2^0)^2 \le R^2, \\ \rho_{max}, & \\ & \text{for} \quad (X_1 - X_1^0)^2 + (X_2 - X_2^0)^2 > R^2 \end{array} \right. \tag{34}$$

This function, which prescribes the initial distribution of the dislocation density, takes a constant value outside and on a given circle of the radius R and centered at (X_1^0, X_2^0), namely $\rho_0^1(X_1, X_2) = \rho_{max}$ for (X_1, X_2) such that $(X_1 - X_1^0)^2 + (X_2 - X_2^0)^2 - R^2 \ge 0$. The maximum dislocation density results at the center of the aforementioned circle, i.e. $\rho_0^1(X_1^0, X_2^0) = \rho_{min}$.

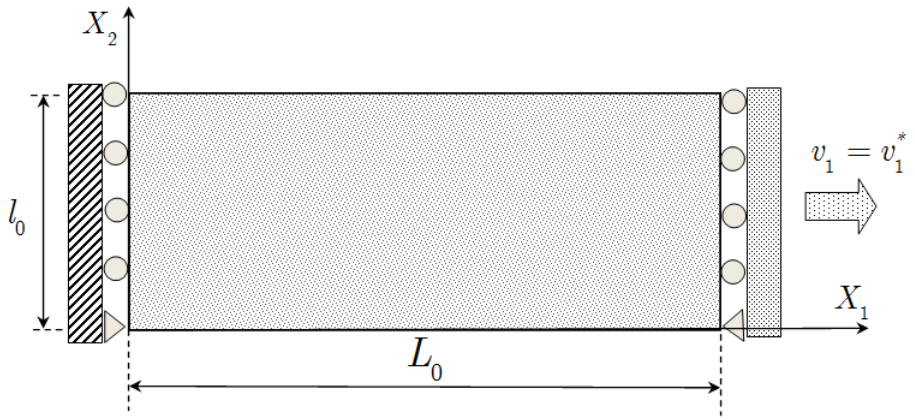

Fig. 1: *Tension problem of single crystal*

The material parameter values are taken from [8] to be: $\mathcal{C}_{11} = 166.1$ GPa, $\mathcal{C}_{12} = 119.9$ GPa, $\mathcal{C}_{44} = 75.6$ GPa, $\mu = 45$ GPa, $\dot{\gamma}_0 = 10^{-3}\ s^{-1}$, $n = 20$, $\rho_{min} = 1400\ mm^{-2}$, $\rho_{max} = 2730\ mm^{-2}$, $b = 2.57 \cdot 10^{-7}\ mm$, $y_c = 0.5 \cdot 10^{-6}\ mm$, $K = 75$, $a^{\alpha\beta} = 0.42$ if $\alpha = \beta$, 0.52 otherwise, $\hat{\rho}_0 = 8.96{\cdot}10^{-3}\ g/mm$, $\zeta_0^\alpha = \mu b \left(\sum_\beta a^{\alpha\beta} \rho_0^\beta \right)^{1/2} + \zeta^*$, $\zeta^* = 34.6{\cdot}10^{-3} GPa$, $L_0 = 50\ mm$ and $l_0 = 20mm$.

For the numerical computations performed, the activation condition $\tau^\alpha \geq \zeta^\alpha$ allows us to emphasize the domains in which the plastic deformation occurs at a given moment. Moreover we suppose that once the element has been activated, it remains active during the loading process.

The finite element mesh used in the present simulation has 426 elements and 238 nodes. To ensure the stability of the time-integration scheme, we use a constant time increment $dt = 0.01s$.

In the beginning of the deformation process, the sheet is fully in an elastic state since no system has been activated, namely $\tau^\alpha < \zeta^\alpha$ for all finite elements, and the stress is homogeneous. At a certain moment, say t^*, the plastic deformation starts from the central zone of the sheet and spreads to the ends of the sheet as it can be seen from Fig.2. In Fig.3 the variation of the plastic shear γ^1 at the points of the sheet is plotted at a certain moment, say $t = 14s$.

As the points of the sheet enter the plastic zone, a small necking appears in the plastic zone, say at moment $t = 14s$, but the phenomenon is not suficiently visible because of the boundary condition imposed on the problem, which allows the glide of the sheet along axis X_2 during the tensile test. On the contrary, if the plastically deformed zone is frozen at a certain moment, say $t = 14s$, then the necking becomes more visible in a continuously developed tensile test.

In Fig.4, the axial component of the Cauchy stress tensor, T_{11}, versus the axial strain, E_{11}, is plotted at a central element of the discretized sheet. The distribution of the dislocation density, ρ^1, on the sheet is presented in Fig.5 at moment $t = 34s$. The solution of the discretized variational problems at moment $t = 34s$ are plotted in Fig.6 and Fig.7, namely the velocity components $v_1 = v_1(x_1, x_2)$ and $v_2 = v_2(x_1, x_2)$ as functions of the points of the sheet.

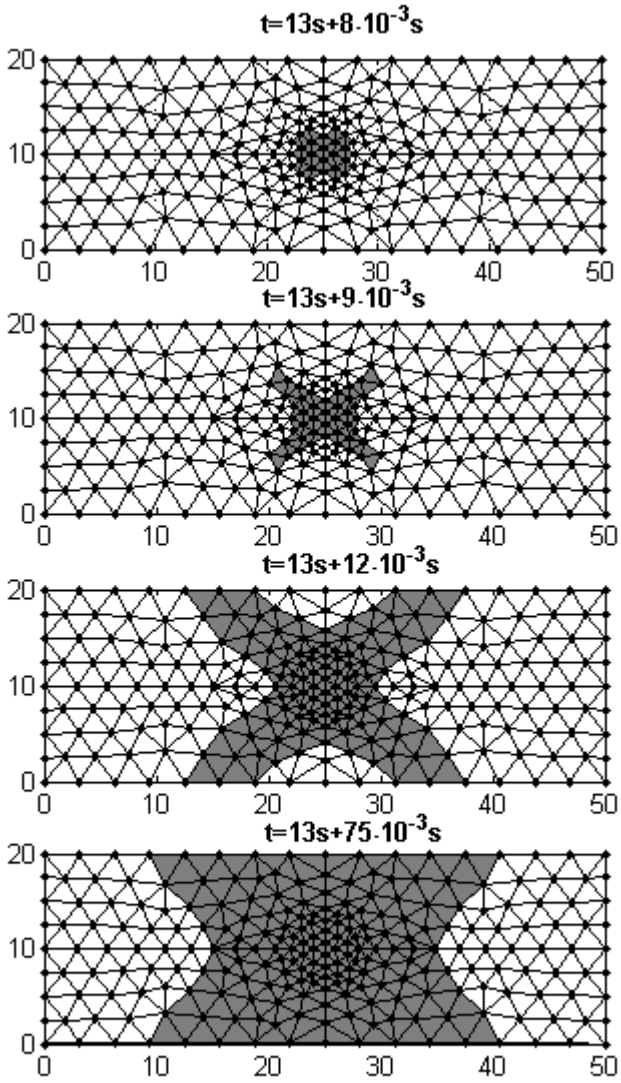

Fig. 2: Plastically deformed zone at different moments

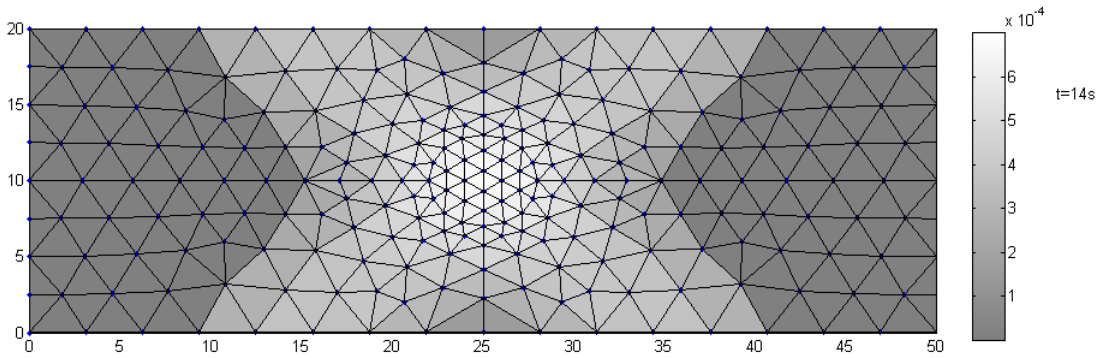

Fig. 3: Distribution of the plastic shears γ^1 in the sheet at time $t = 14s$.

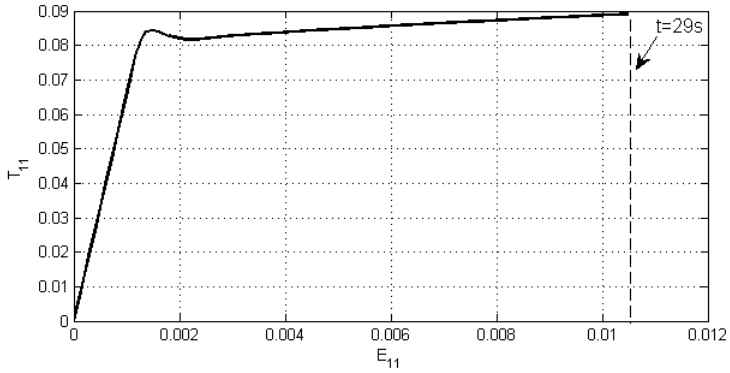

Fig. 4: Axial stress T_{11} versus E_{11} at a central element of the sheet at time $t = 34s$.

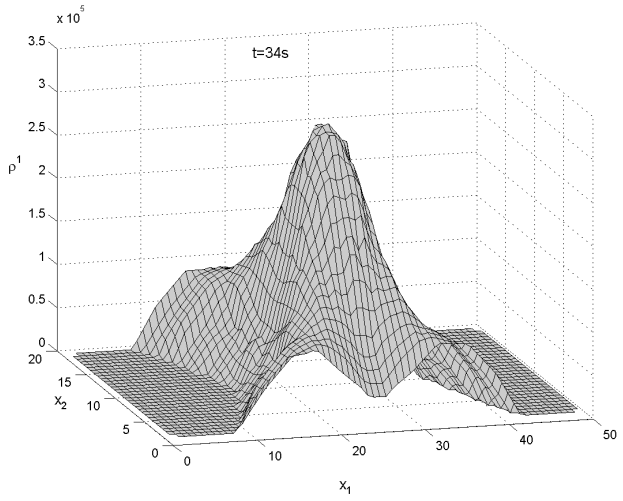

Fig. 5: Distribution of the dislocation density $\rho^1 = \rho^1(x_1, x_2)$ on the points of the sheet, at the moment $t = 34s$.

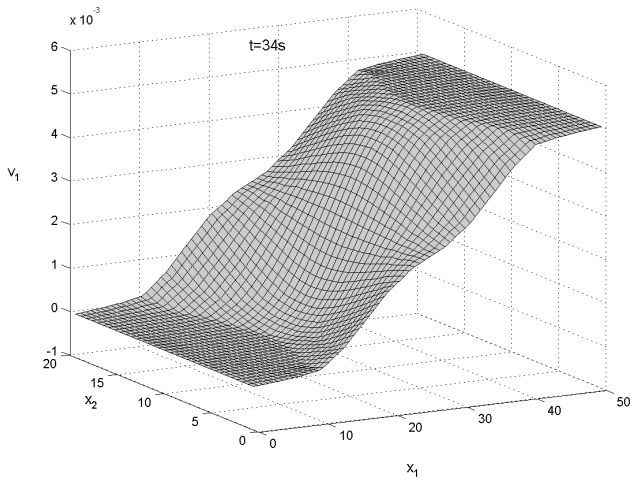

Fig. 6: Velocity field $v_1 = v_1(x_1, x_2)$ at moment $t = 34s$.

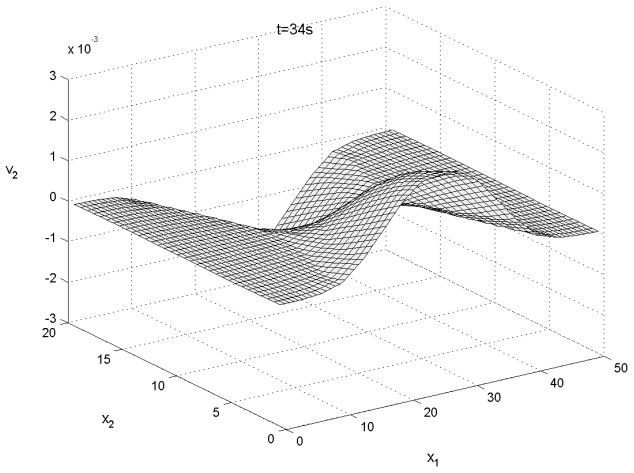

Fig. 7: Velocity field $v_2 = v_2(x_1, x_2)$ at the moment $t = 34s$.

Acknowledgments. The authors acknowledge the support received from the Romanian Ministry of Education, Research and Innovation, through PN II--IDEI--PCCE Programme, Contract no. 100/2009.

References

[1] L. Bortoloni and P. Cermelli: Journal of Elasticity 76 (2004), p.113

[2] M. Kuroda: Int. J. Solid Struct. 48 (2011), p. 3382

[3] M. Kuroda and V. Tvergaard: Int. J. Solid Struct. 56 (2008), p. 2573

[4] S. Cleja-Ţigoiu and E. Soós: Applied Mechanics Reviews 43 (1990), p.131

[5] S. Cleja-Ţigoiu: European Journal of Mechanics - A/Solids (1996), p. 761

[6] S. Cleja-Ţigoiu: Rendiconti del seminario matematico, Univ. Pol. Torino, 58 (2000), p. 69

[7] S. Cleja-Ţigoiu and R. Paşcan: Mathematics and Mechanics of Solids (2012) DOI: 10.1177/1081286512439060.

[8] C. Teodosiu and J.L. Raphanel, in *Large Plastic Deformations, Fundamental Aspects and Applications to Metal Forming*, edited by Teodosiu, Raphanel and Sidoroff, Brookfiels, Rotterdam (1993).

[9] C. Teodosiu and F. Sidoroff: Int. J. Engn. Sci. 14 (1976), p. 165

[10] T.C.T. Ting, *Anisotropic Elasticity* (Oxford University Press 1996).

[11] S. Ha, K. Kim: Mathematics and Mechanics of Solids, (2011), p. 651

[12] S. Cleja-Ţigoiu, R. Paşcan and N. Stoicuţă, in *Inverse problems and computational mechanics*, edited by L. Marin, L. Munteanu, V. Chiroiu, Ed. Academiei Române (2011)

[13] T.J.R. Hughes, *The Finite Element Method. Linear Static and Dynamic Finite Element Analysis* (Prentice-Hall, Inc., Englewood Cliffs, New Jersey 07632, 1987).

[14] L.J. Segerlind, *Applied Finite Element Analysis* (John Wiley and Sons, New York 1984).